MIT, 1990.
[5] Streckwall H., "Hydrodynamic Analysis of Three Propellers Using a Surface Panel Method for Steady and Unsteady Inflow Conditions", 22nd ITTC Propulsion Committee, 1998, France.
[6] Idris B.M., Marou H., and Ikehata M., "Theoretical Analysis of Unsteady Characteristics of Marine Propeller in Ship's Wake", Journal of Society of Naval Architects of Japan, 1984, 156,. 60-68
[7] Takahashi M. and Oku M., "The Cavitation Characteristics of MAU Type Propeller, 2nd report: Pressure Distribution on Blade Surface in Non-Uniform Flow", Journal of Society of Naval Architects of Japan, 1978, 143, 61-67
[8] Kinnas A.S. and Hsin C.Y., "A Potential Based Panel Method for Unsteady Flow Around Open and Ducted Propellers", Proceedings of 18th Symposium on Naval Hydrodynamics, 1991, Korea.
[9] Kerwin, J.E. and Lee C.S., "Prediction of Steady and Unsteady Marine Propeller by Numerical Lifting Surface Method", SNAME Transactions, 1987, 86, 218-253.
[10] Morino L. and Kuo C.C., "Subsonic Potential Aerodynamics for Complex Configuration: A general Theory", AIAA Journal, 1974, 12 (2), 191-197.
[11] Morino L., Chen L.T. and Suciu E.O., "Steady and Oscillatory Subsonic Aerodynamics Around Complex Configuration", AIAA Journal, 1975, 13.
[12] Ghassemi H. Ikehata M. and Yamazaki H., "An Investigation of Wake Models and Its Effects on Hydrodynamic Performance of Propeller by Using of Surface Panel Method", Journal of Society of Naval Architects of Japan, 1995, 178.
[13] Breslin J.P. and Andersen P., "Hydrodynamics of Ship Propellers", Cambridge Ocean Technology Series 3, 1994.
[14] Ukon Y., et.al, "Measurement of Pressure Distributions on a Full Scale Propeller-Measurement on a Highly Skewed propeller", Journal of Society of Naval Architects of Japan, 1991, 170, 111-123.
[15] Koyama K., "Application of a Panel Method to the Unsteady Hydrodynamic Analysis of Marine propellers", Proceedings of the 19th Symposium on Naval Hydrodynamics, 1992, Korea.
[16] Ohkusu M., "Advances in Marine Hydrodynamics, Chapter 6, Theory and Numerical Methods for the Hydrodynamic Analysis of Marine propellers", Computational Mechanics Publications, 1996, 279-322.
[17] Lee J.T., "A Potential Based Panel Method for the Analysis of Marine Propeller in Steady Flow", Ph.D. Dissertation, MIT 1987,
[18] Ukon Y., Kudo T., Yuasa H., Kamiirisa H., "Measurement of Pressure Distribution on Full Scale Propellers", Proceedings of the proepllers/Shafting'91 Symposium, The Society of naval Architects and marine Engineers, 1991, Virginia Beach.
[19] Ghassemi H., "A study on Hydrodynamic Analysis of Propellers and Cavitation Prediction of Hydrofoils by the Application of Surface Panel Method", Ph.D. Dissertation,, Yokohama National University, 1997, Yokohama, Japan.
[20] Hess J.L. and Smith A.M.O., "Calculation of Non-lifting Potential Flow about Arbitrary 3-Dimensional Bodies", Journal of Ship Research, 1964, 8 (2), 22-44.
[21] Yanagizawa M., "Calculation for Aerodynamics Characteristics on a 3-D Lifting Bodies in Subsonic Flow Using Boundary Element Method", TR of National Aerospace Laboratory, TR-835, 1984.
[22] Yamazaki, H. and Ikehata M., "Numerical Analysis of Unsteady Open Characteristics of Marine Propeller by Surface Vortex Panel Method", Journal of Society of Naval Architects of Japan, 1995. 178.
[23] Marou H., Ikehata M. and Ando M., "Theoretical Prediction of Unsteady Propeller Characteristics in the Non-Uniform wake Field", Proceedings of the 15th Symposium on Naval Hydrodynamics, Hamburg, Germany.
[24] Newman J.N., "Distributions of Sources and Normal Dipoles over a Quadrilateral Panel", J. of Engineering Mathematics, 1986, 20, 113-126.
[25] Hsin C.Y., Kerwin J.E., Kinnas S.A., "A Panel Method for the Analysis of the Flow Around Highly Skewed Propellers", Proceedings of the Propllers/Shafting'91 Symposium, 1991, Virginia.
[26] Kinnas S.A. and Hsin C.Y., "Boundary Element Method for the Analysis of the Unsteady Flow around Extreme Propeller Geometry", AIAA, Journal, 1992, 30 (3).
[27] Ghassemi H., "Boundary Element method Applied to the Cavitating Hydrofoil and Marine propeller", to be published to the Journal of Oceanic Engineering International, 2000.

non-uniform flow.

Acknowledgements

The author would like to thank to NSERC (Natural Sciences and Engineering Research Council) of Canada for a grant-in-aid of this research. He also appreciated to the guidance given to him by Prof. Neil Bose of Memorial University of Newfoundland, Dr. David Molyneux of IMD/NRC, Canada, and Prof. Kuniharu Nakatake of the Kyushu University, Japan. Their kind encouragement, useful discussions, comments and provisions of relevant references were essential to the development of this paper.

Nomenclature

$A^k{}_{jm}$	Jacobian matrix
D	propeller diameter
J	advance coefficient
k	blade index
K	number of propeller blades
K_t, K_{FY}, K_{FZ}	Thrust coefficients
K_q, K_{MY}, K_{MZ}	moments coefficients
L	time step index
N_{tot}	total panel on propeller
M	number of radial panels
N	number of chordwise panels
N_W	number of panels on wake surface
F_X, F_Y, F_Z	forces on propeller
M_X, M_Y, M_Z	moments on propeller
$\vec{n}$	outward normal unit vector
n	number of propeller revolutions
p_∞	static pressure
$p(t)$	pressure on the body surface
S_B	surface on propeller
S_W	surface on trailing vortex wake
s/C	fraction of chord
$\vec{V}_A$	advance velocity
$\vec{V}(t)$	total tangential velocity to the body
$\vec{V}_I$	resultant inflow velocity
V_S	ship speed
$\vec{V}_W$	inflow wake velocity
$\vec{v}(p)$	induced velocity at any field point
Q	propeller torque
T	propeller thrust
w	wake fraction
$\vec{X}_P$	position vector on propeller
ρ	mass density of fluid
Δt	time interval
$\Delta\theta_W$	angular interval
ω	measured axial mean velocity
Γ	non-dimensional circulation at TE
ϕ_I	inflow velocity potential
ϕ	perturbation velocity potential
Φ	total velocity potential
$\partial\phi/\partial n$	normal derivative of potential
$\partial\phi/\partial t$	time derivative of potential
$C^k{}_{ij}, W^k{}_{ijl}$	dipole influence coefficients
$S^k{}_{ij}$	source influence coefficients
$\nabla C^k{}_{ij}, \nabla W^k{}_{ijl}$	gradient dipole influence coefficients
$\nabla S^k{}_{ij}$	gradient source influence coefficient

References

[1] Hoshino T., "Hydrodynamic Analysis of Propellers in Steady Flow Using a Surface Panel method", Journal of Society of Naval Architects of Japan, 1989, 165, 55-70.

[2] Hoshino T., "Hydrodynamic Analysis of Propellers in Unsteady Flow Using a Surface Panel method", Journal of Society of Naval Architects of Japan, 1993, 174, 79-92.

[3] Ando J., Maita S. and Nakatake K., "A New Surface Panel Method to Predict Steady and Unsteady Characteristics of Marine Propeller", 22nd Symposium on Naval Hydrodynamics, 1998, Washington D.C.

[4] Hsin C.Y., "Development and Analysis of Panel Methods for Propellers in Unsteady Flow", Ph.D. Dissertation,

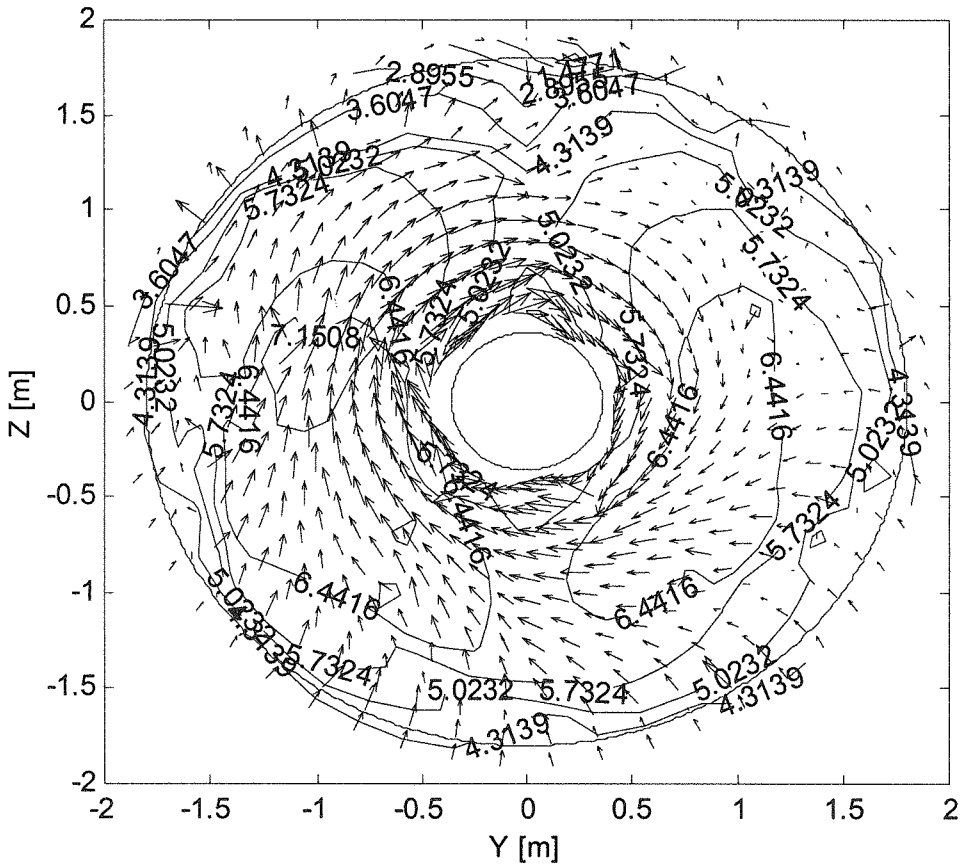

Figure (17) Induced axial and cross velocities behind the propeller Seiun-Maru HSP at x/D=0.5, J=0.851.

4-Conclusions

A steady and unsteady potential-based BEM was presented for the analysis of the hydrodynamic performance of marine propellers subject to non-uniform wake flow. An efficient algorithm of explicit Kutta condition (at blade trailing edge) has been implemented in order to ensure faster convergence at each time step.

From the above numerical analysis, the following conclusions can be drawn:

The method can evaluate accurately the hydrodynamic performance of the propeller in the steady flow as well as unsteady flow.

The iterative Kutta condition is indispensable to solve the steady and unsteady propeller problem and it was found that the present Newton-Raphson method was very efficient to guarantee the almost equal pressure at the trailing edge.

The unsteady propeller forces and moments can be predicted with reasonable accuracy by the present method.

The total thrust and torque of the conventional propeller give slightly bigger fluctuating than the highly skewed propeller.

The present method can predict the induced velocity and flow field behind the propeller. It is recommended to get some measurement the flow velocity behind the propeller operating in the

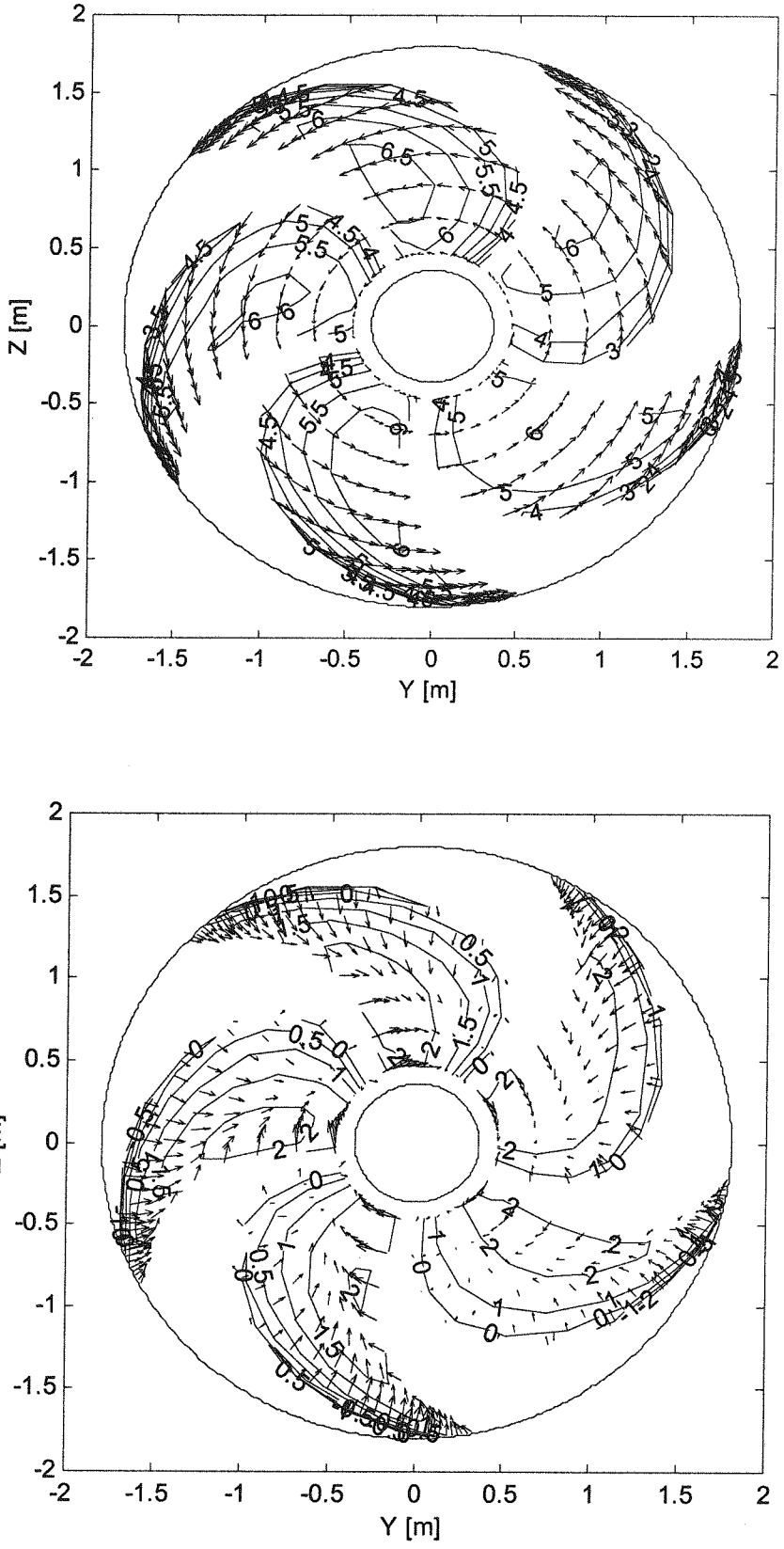

Figure (16) Induced cross and axial velocity on back side (up) and face side (down) of Seiun-Maru HSP, J=0.851.

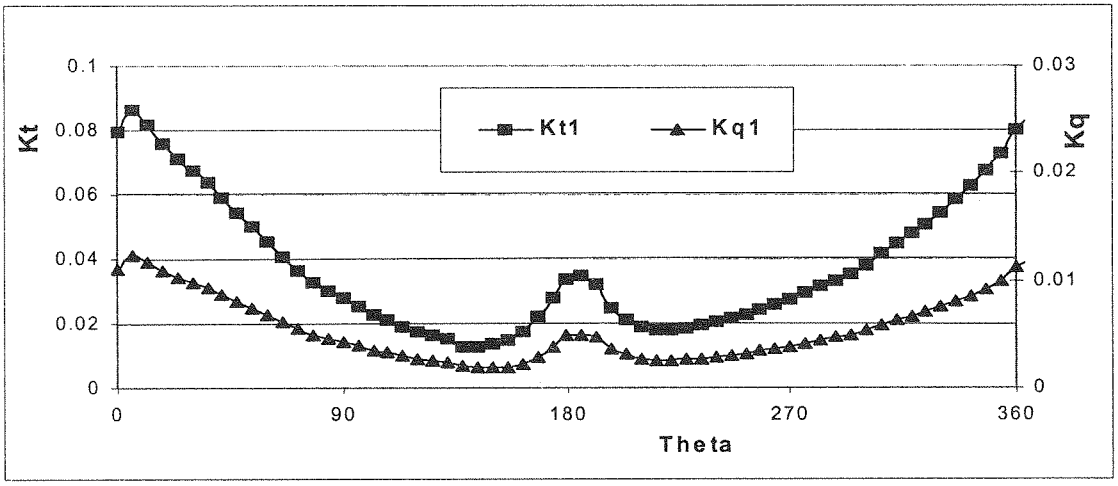

Figure (14) One blade thrust and torque fluctuations for Seiun-Maru CP *Kt=0.172.*

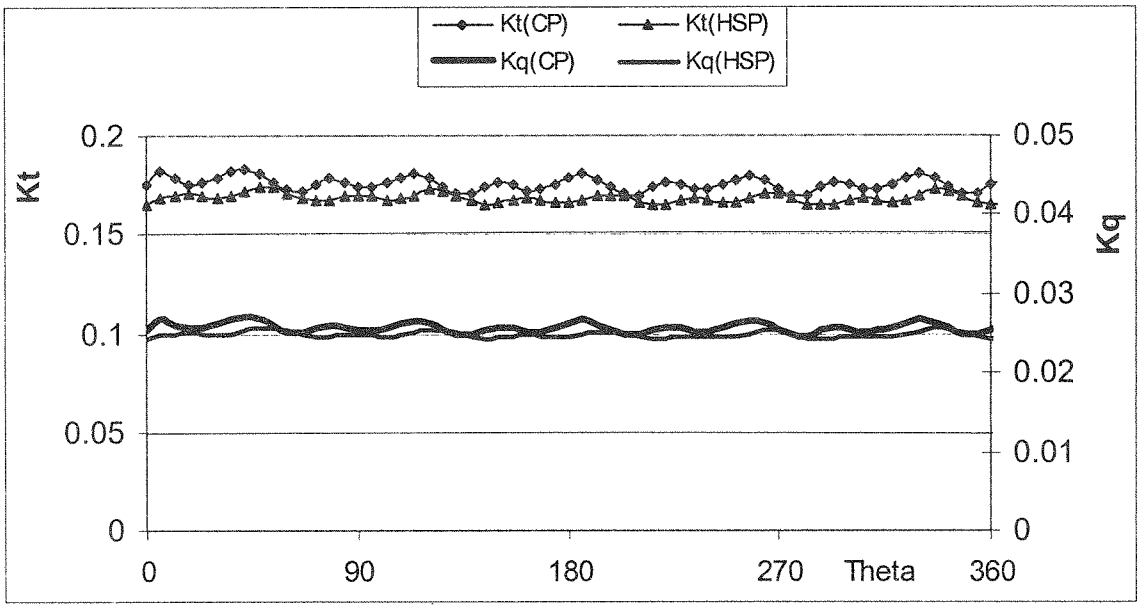

Figure (15) Total thrust and torque fluctuations for Seiun-Maru CP and HSP, *Kt=0.172.*

3-4-Velocity Field Around the Marine Propeller

In order to show induced velocity generated by the propeller, the axial and cross velocity vectors on the propeller surface and a position behind propeller are determined.

Calculated axial and cross induced velocities on both sides of the HSP propeller is shown in Figure 16.

In Fig. 17 the plane on which the velocity components are computed is located at (*X/D=0.5*) downstream behind the propeller. For further judgement on these results, experimental data are required to compare with simulation results.

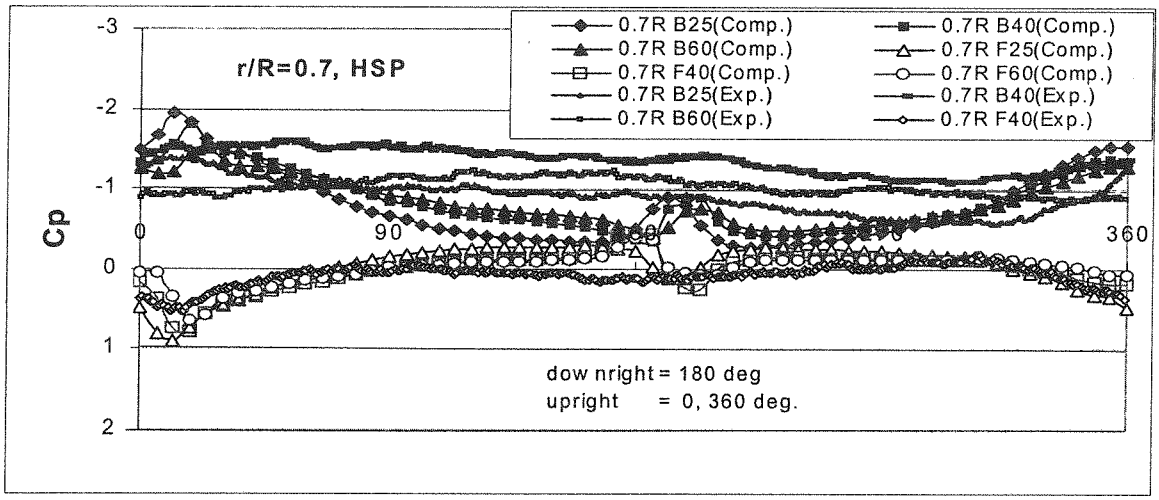

Figure (11) Fluctuating pressure for Seiun-Maru HSP on 0.7R, *Kt=0.172.*

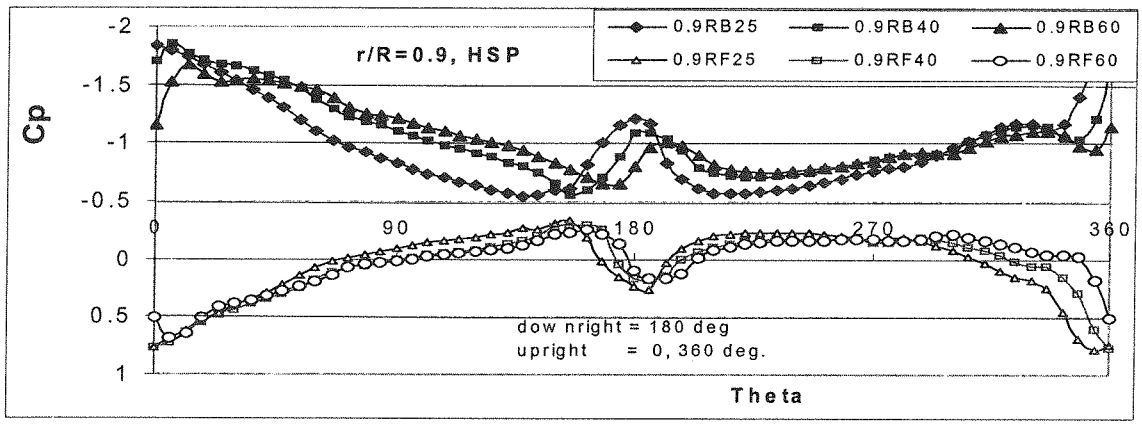

Figure (12) Fluctuating pressure for Seiun-Maru HSP on 0.9R, *Kt=0.172.*

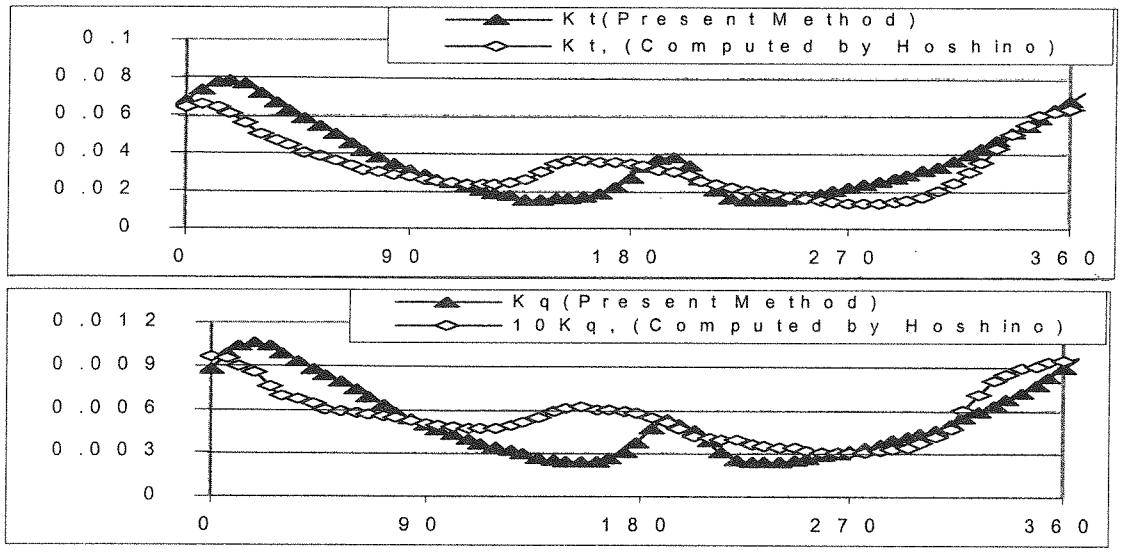

Figure (13) One blade thrust and torque fluctuations for Seiun-Maru HSP, *Kt=0.172.*

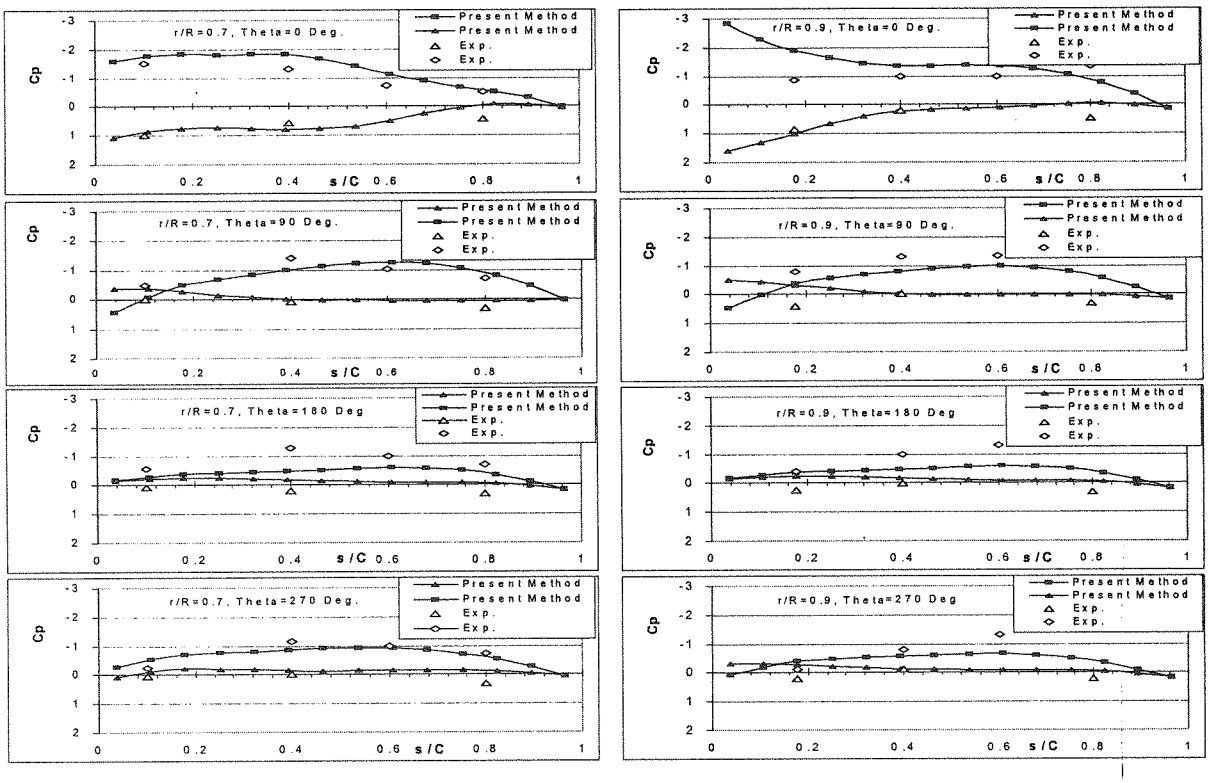

Figure (9) Comparison of chordwise pressure distribution for HSP at various rotating angle, *J=0.851.*

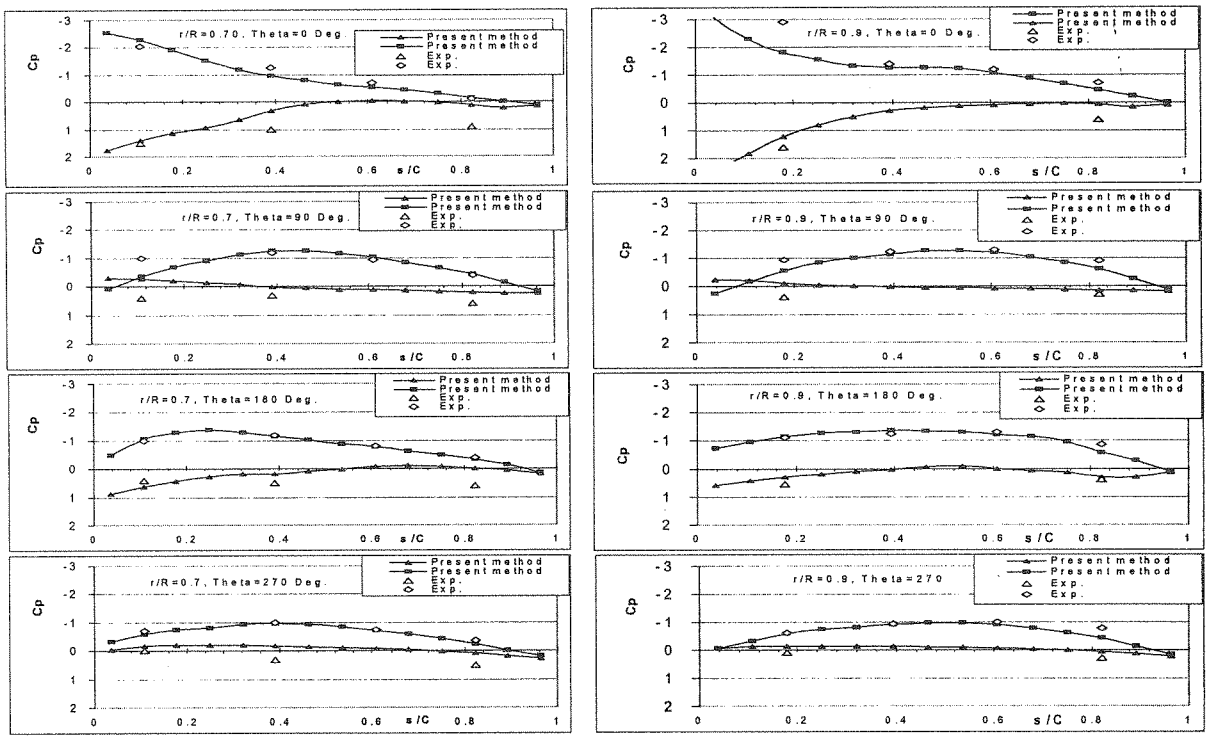

Figure (10) Comparison of chordwise pressure distribution for CP at various rotating angle, J=0.851.

For the *Kt=0.172* condition the calculated one blade thrust and torque is given in Fig. 13 with Hoshino's results as a function of the blade angular position (*0-360*) degrees for one cycle. The angle is zero at upright position and runs clockwise if one looks from behind. Fig 14 also shows the results for CP with the same tendency of the HSP, in which small humps appearing in both K_t and K_q with present method may be caused by the tangential inflow components, which shows pronounced jumps at angular position equal to *0* and *180* degrees.

Chordwise pressure distributions at various angular positions of 0, 90, 180 and 270 degrees at 0.7R and 0.9R radial sections are compared to the experimental data are shown in Figs. 9 and 10.

In Fig. 11 and 12, the pressure at certain points at 0.7R and 0.9R is plotted as a function of the blade angular position (0~360). The pressure results from the present method show quiet pronounced fluctuating but the measure values are smooth in every case.

Total thrust and torque fluctuations for Seiun-Maru CP and HSP propellers are shown in Fig. 15. It can clearly be seen that fluctuating of conventional propeller gives significantly bigger fluctuating than the highly skewed propeller at the same operating condition. Therefore, the HSP propeller may help to avoid the noise and vibration rather than CP propeller.

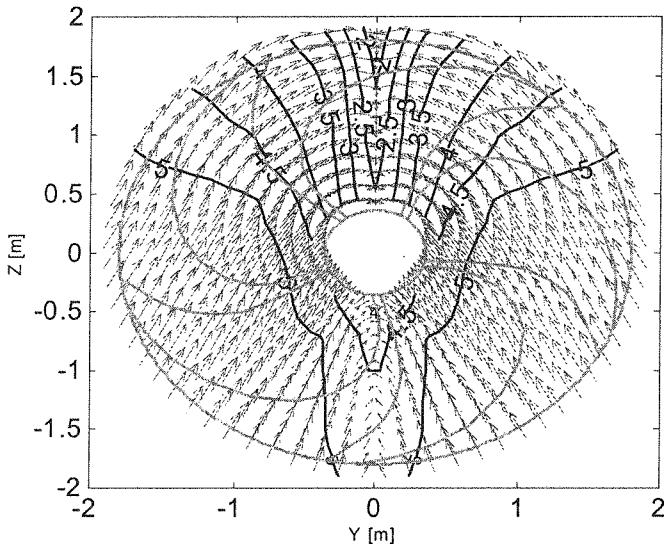

Figure (7) Wake flow velocity distribution for Seiun-Maru HSP.

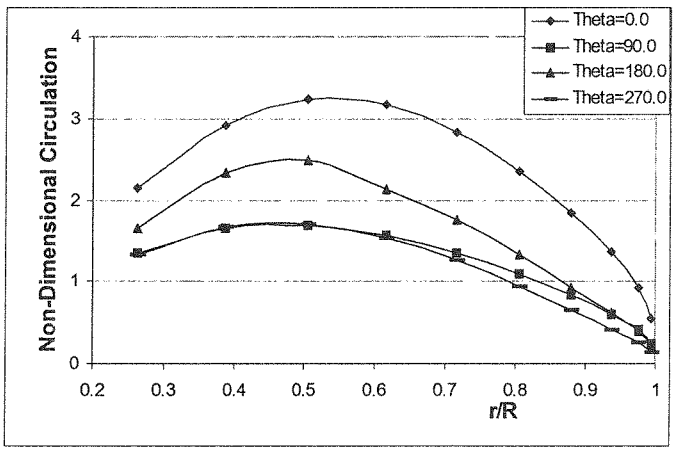

Figure (8) Circulation distributions on one blade during one revolution of HSP, *J=0.851.*

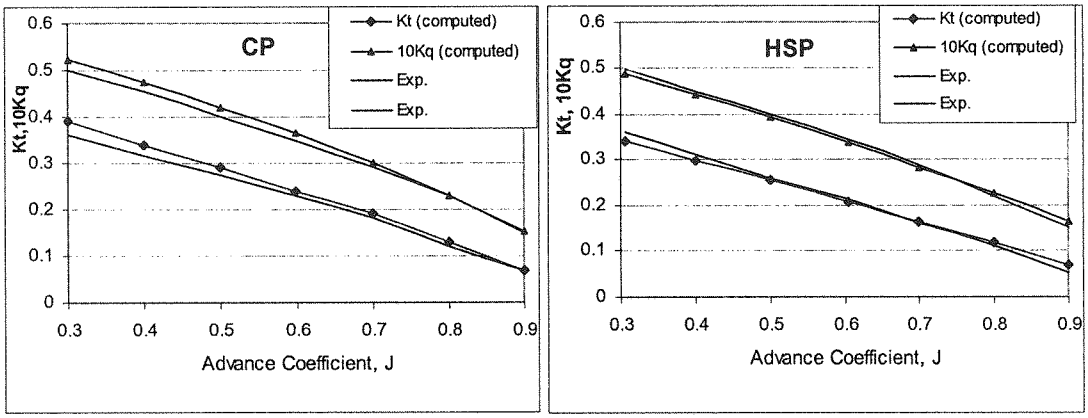

Figure (5) Open water characteristics of HSP and CP propellers.

3-3-Unsteady Flow

Data for the same propellers (but in full-scale) of CP and HSP Seiun-Maru were obtained for the unsteady flow condition full scale on the training ship of SRI and carried out by Ukon et al. [18]. All principal particulars of both propellers are the same as the model, except the diameter, as given in Table 1. Estimated measured wake flow in the full scale is shown in Fig. 7. Not only the axial component but also the tangential and radial components are taken into consideration in the present calculations.

The panel arrangement of the HSP propeller and its wake at third step ($\theta_W = 18\text{deg.}, \Delta\theta_W = 6\text{deg.}$ (is shown in Fig. 6. The unsteady panel calculations on the HSP and CP were also performed with 14 panels in chordwise and 12 panels in radial. Hub also divided by total panel (20*28) which 28 in axial and 20 in circumferential directions.

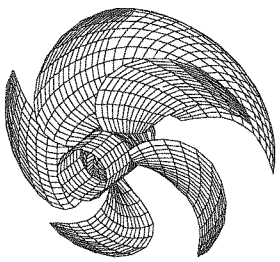

Figure (6) Panel Arrangement for a HSP propeller and its wake at third step ($\theta_W = 18\text{deg.}, \Delta\theta_W = 6\text{deg.}$)

Fig. 8 shows non-dimensional circulation distributions on one blade of the HSP propeller during one revolution at J=0.851. As shown in this figure, bigger circulation values were obtained at upright position where larger loading occurred.

The blade surface pressure distributions have been measured at 0.7R and 0.9R spanwise locations on the pressure and suctions sides. For the present calculation the procedure used K_t identity based on ship speed to determine the operating conditions in the calculations. Ship speed was varied until the required thrust coefficient value $Kt=0.172$ was achieved.

Figure (2) Panel arrangement of HSP (left) and CP (right) Seiun-Maru propellers.

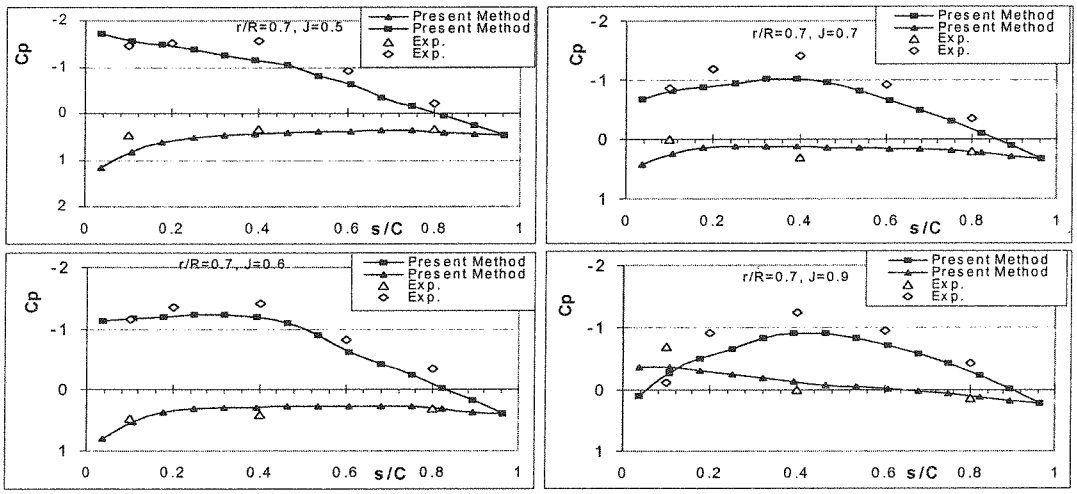

Figure (3) Comparison of pressure distribution at r/R=0.7 for Conventional Propeller (CP).

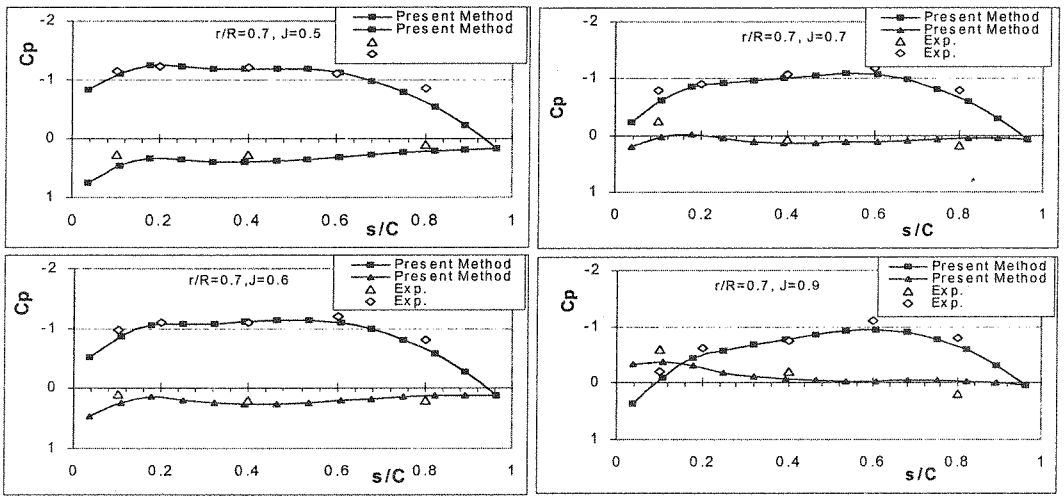

Figure (4) Comparison of pressure distribution at r/R=0.7 for Highly Skewed Propeller (HSP).

Propeller Type	CP	HSP
Diameter (full scale) [m]	3.6	3.6
Diameter (model) [m]	0.400	0.400
Exp. Area Ratio	0.65	0.70
Pitch Ratio at 0.7R	0.95	0.944
Boss Ratio	0.1972	0.1972
No. of Blades	5	5
Blade thickness ratio	0.0442	0.0496
Rake Angle [deg]	6.0	-3.03
Skew Angle [deg.]	10.5	45.0
Blade Section	MAU	Modified SRI-B

Table (1) Main dimensions of the propellers

CPU time for these panel calculations (at one operating condition) was about 50 hours by PC Pentium 500 MHz processor for 180 time steps (three revolutions of the propeller). Most CPU time is required for the convergence of the Kutta condition at the trailing edge. A very effective numerical technique was used to decrease the iterative Kutta condition to converge faster. It was noted that at each iterative Kutta condition, the system of equations should be solved $K*M$ (5*12=60) times at each time step. It can be imaged that the Kutta condition is very time consuming in the unsteady flow. In the following sub-section, numerical results in the steady and unsteady flows are discussed.

3-2-Steady Flow

Although several lifting surface methods have successfully predicted propeller forces in steady and unsteady flows, they are not able to calculate pressure distribution accurately. The present method is able to predict the pressure distribution more accurately since the singularities are distributed on a real blade surface.

For the present method, calculated results of pressure distribution are compared to the experimental data for both the CP and HSP propellers. The HSP propeller is a 0.400-m diameter 5-bladed propeller with maximum skew at the tip is 45 degrees and a sophisticated blade section.

The trailing vortex wake leaves the trailing edge of the blade and flows into the slipstream with the local velocity at that position. Details of the vortex wake model were investigated by the author [12] and found that a deformed wake model based on the thrust loading condition gives better results of the hydrodynamic characteristics of the propeller which matched the present research.

The surface pressure distribution is one of the most essential parameters for design and analysis of the marine propeller. Chordwise pressure distributions at 0.7R calculated by the present method are compared in Figs 3 and 4 with equivalent experiment data for the CP and HSP propellers. The agreement between the experiment and calculated results is especially good at the design loading conditions of $J=0.6$, and reasonably good at all other loading conditions, for both CP and HSP designs.

The computed open-water characteristics of the propellers are compared with the experimental data in Figure 5. Values of computed thrust K_t and torque coefficients K_q of the CP and HSP propellers give in good agreement with experimental data.

In the steady calculations, The hydrodynamic characteristics of the propeller are obtained as given below:

$$J=\frac{V_A}{nD},\quad K_t=\frac{T}{\rho n^2 D^4},\quad K_q=\frac{Q}{\rho n^2 D^5} \tag{21}$$

2-4-Calculation of Flow Field Velocity Around the Propeller

From Green's theorem in the potential field, equation (5), we can alternatively construct in the velocity field. Taking the gradient of the perturbation velocity potential at any field point, the induced velocity which can be expressed as;

$$4\pi\vec{v}(p,t)=\int_{S_B}\left\{\phi(q,t)\nabla_p\frac{\partial}{\partial n_q}\left(\frac{1}{R(p;q)}\right)-\frac{\partial\phi(q,t)}{\partial n_q}\nabla_p\left(\frac{1}{R(p;q)}\right)\right\}dS+\int_{S_W}\Delta\varphi(q,t)\nabla_p\frac{\partial}{\partial n_q}\left(\frac{1}{R(p;q)}\right)dS \tag{22}$$

Here, from the discretization of the body and wake, and assuming the potential ϕ and the value of $\frac{\partial\phi}{\partial n}$ are constant within each panel. Then, equation (22) can be written by;

$$\vec{v}(p)=\sum_{k=1}^{K}\sum_{j=1}^{N_{tot}}(\phi_j)\nabla_p C^k{}_{ij}+\sum_{k=1}^{K}\sum_{j=1}^{M}(\Delta\Delta\varphi_j)\nabla_p W^k{}_{ijl}+\sum_{k=1}^{K}\sum_{j=1}^{N_{tot}}\left(\frac{\partial\phi}{\partial n}\right)_j^k\nabla_p S^k{}_{ij}\qquad i=1,2,\ldots,N_{tot} \tag{23}$$

where $\nabla_p C^k{}_{ij}$, $\nabla_p W^k{}_{ijl}$ and $\nabla_p S^k{}_{ij}$ are the velocity influence coefficients. Those coefficients can be evaluated analytically by Morino's method [11] by assuming that the surface elements are approximated by a number of quadrilateral hyperboloidal panels.

Calculations of the velocity influence were more sensitive than the potential coefficient, and also the required storage was three times more than the storage of the potential coefficient. There was one big advantage that the velocities can directly be obtained for any field points.

3-Numerical Results and Discussion

3-1-Propeller Type

In order to evaluate the accuracy and the applicability of the present method, two different propeller models were selected. For both propellers, very precise measurements of the blade surface pressure were conducted. Both propellers have 5 blades. One is a conventional design with MAU sections and the other is a highly skewed propeller with modified SRI-b sections. Principal particulars of the propellers are shown in Table 1.

In the steady calculations, the model propellers were discretized with (*M=12*) in radial and (*N=14*) in chordwise direction so the total number of panels was 336 per blades plus a hub with (4*28=112) panels per segments. The total number of panels for the steady calculation was 448 on the key blade. The potential and pressure distributions on the other blades were taken as equal to the key blade. Panel arrangements of the propellers are shown in Fig. 2.

For unsteady flow, each blade is subject to the different non-uniform wake velocity, the potential and pressure distribution have to be calculated at each time step. The System of equations is *K* times larger than steady flow. We tried to keep the panel pattern the same as for the steady condition, which gave the total number of panels for all blades and hub to be 2240.

$$\frac{\Delta\varphi}{\Delta t}=\frac{4\phi\phi(L-3\phi\phi(-1)+\phi(L-2)}{2\Delta\Delta} \tag{17}$$

The pressures were finally expressed in terms of the non-dimensional pressure coefficient as

$$C_p=\frac{p(t)-p_\infty}{1/2\,\rho/^2 D^2} \tag{18}$$

where n is the rotational speed of the propeller and D is the diameter of the propeller.

The unsteady forces F_X,F_Y,F_Z and moments M_X,M_Y,M_Z acting on a propeller can be obtained by integrating the unsteady pressures over the blade and hub surfaces. They are expressed on the fixed coordinate system (X,Y,Z) as;

$$\begin{aligned}
&F_X(t)=-T(t)=\int_S (p(t)-p_\infty)n_x ds\\
&F_Y(t)=\int_S (p(t)-p_\infty)(n_y\cos(\omega os-n_z\sin(\omega in(\omega t\\
&F_Z(t)=\int_S (p(t)-p_\infty)(n_z\cos(\omega os-n_y\sin(\omega in(\omega t\\
&M_X(t)=Q(t)=\int_S (p(t)-p_\infty)(n_y z-n_z y)ds\\
&M_Y(t)=\int_S (p(t)-p_\infty)\left[(n_z x-n_x z)\cos(\omega)c+(n_x y-n_y x)\sin(\omega)si\right]ds\\
&M_Z(t)=\int_S (p(t)-p_\infty)\left[(n_x y-n_y x)\cos(\omega)c+(n_x z-n_z x)\sin(\omega)si\right]ds
\end{aligned} \tag{19}$$

where $\vec{n}(n_x, n_y, n_z)$ is outward normal vector on propeller. $T(t)$ and $Q(t)$ are thrust and torque of the propeller.

Adding the viscous components to the above forces and moments given by Prandtl-Schlichting formula [12], we finally obtain the total unsteady propeller forces and moments. Then, the non-dimensional coefficients of the unsteady propellers and forces and moments were expressed as follows:

$$\begin{aligned}
&K_t(t)=\frac{T(t)}{\rho n^2 D^4}, \qquad K_q(t)=\frac{Q(t)}{\rho n^2 D^5}\\
&K_{FY}(t)=\frac{F_Y(t)}{\rho n^2 D^4}, \qquad K_{MY}(t)=\frac{M_Y(t)}{\rho n^2 D^5}\\
&K_{FZ}(t)=\frac{F_Z(t)}{\rho n^2 D^4}, \qquad K_{MZ}(t)=\frac{M_Z(t)}{\rho n^2 D^5}
\end{aligned} \tag{20}$$

jump $\Delta\phi_j^k(L)$ can be determined by Newton-Raphson iterative scheme as expressed in equation (14) and it is found that the Newton-Raphson procedure was very effective to guarantee the equal pressure at the trailing edge. If consequently, $\Delta p_j^k(L)$ is not equal at TE, we proceed to another iteration with $\Delta\phi_j^k(L)$ determined as follows:

$$\Delta\phi^k{}_{j1}(L)^{(n+1)} = \Delta\phi^k{}_{j1}(L)^{(n)} - \sum_{m=1}^{M} \left(A^k{}_{jm}(L)\right)^{-1} \Delta p^k{}_{m}(L)^{(n)}, \quad j=1,2,\ldots M \tag{14}$$

where n denotes the iteration number and $A^k{}_{jm}(L)$ is the Jacobian matrix which can be expressed as:

$$A^k{}_{jm}(L) = \frac{\partial(\Delta\Delta^k{}_m(L))}{\partial(\Delta\Delta^k{}_{j1}(L))} \tag{15}$$

To save computational time at each time step, we consider the derivative matrix to be constant at any time step and iteration. At each time step L, a new wake panel column is emitted from trailing edge of the blade and all the existing wake panels are shifted downstream by the angular interval $\Delta\theta_W$. Each wake panel keeps the value of the potential jump that received at the time step it was created, in order to ensure that the velocity is considered to be continuous (or without any pressure discontinuity) on the wake surface, as required by equation (7).

The process of time stepping is continued through several propeller revolutions until a steady state oscillation of the potential is achieved. From the experience with calculation method, it was found that three revolution of the propeller were enough to obtain the ultimate oscillatory pattern. Thus, the unsteady pressure distribution and the unsteady propeller force and moments were calculated when the results converged.

It is found that 60 time steps per revolutions of the propeller $\Delta\theta_W = 6$ degrees was enough and the results were accurate, although the results could be improved if the number of time steps was increased to 120 ($\Delta\theta_W = 3$ degrees). However, the effect of the angular interval $\Delta\theta_W$ on the calculation of the thrust of one blade was not large. Therefore, the angular interval of the 6 degrees was commonly used in the present calculations.

2-3-Unsteady Pressure and Hydrodynamic Forces

One the perturbation potential was found, the unsteady pressure distribution on the propeller blade is calculated by the unsteady Bernoulli's equation expressed as;

$$p(t) = p_\infty + \frac{1}{2}\rho\left(|V_I(t)|^2 - |V(t)|^2\right) - \rho\frac{\partial\phi(t)}{\partial t} \tag{16}$$

where the parameters are defined in the nomenclature.

The time derivative of the potential, $\frac{\partial\phi}{\partial t}$, in equation (16) is inherent in the unsteady flow and can be obtained by third-order finite difference scheme as;

discretized into equal intervals Δt. The trailing vortex wake starts from the blade trailing edge and flows downstream of the propeller along the prescribed helical surface by interval $\Delta\theta_W$ as follows:

$$\Delta\theta_W = \omega\Delta t \tag{10}$$

On each of the quadrilateral panels, the dipole and source distributions are approximated by constant strength distributions. Discretization of equation (5) leads to a linear system of algebraic equations for the unknown ϕ at each time step $L = t/\Delta t$ as:

$$2\pi\phi_i(L) = \sum_{k=1}^{K}\sum_{j=1}^{N_{tot}} D^k_{ij}(\phi^k_j(L)) + \sum_{k=1}^{K}\sum_{j=1}^{M}\sum_{l=1}^{N_W} W^k_{ijl}(\Delta\Delta^k_j(L)) + \sum_{k=1}^{K}\sum_{j=1}^{N_{tot}} S^k_{ij}\left(\frac{\partial\phi}{\partial n}\right)^k_j(L) \qquad i=1,2,..N_{tot} \tag{11}$$

where D^k_{ij} , W^k_{ijl} (dipole distributions on body and wake surfaces) and S^k_{ij} (source distribution on body) are influence coefficients on panel j acting on the control point of panel i. Those influence coefficients are nearly evaluated analytically by Morino [10]. The use of quadrilateral surface panels instead of planar panels has been found to be important for the convergence of the present potential based boundary element method. It is found to be especially so when applied to the highly skewed propeller and twisted shape.

The system of equations (11) must be solved at each time step L with respect to the potentials on the all blades. But the influence coefficients are determined on the key blade and re-arranged for all blades in the full matrix form. This is more efficient than calculating influence coefficients for all blades. This system of equation can be written in a matrix form as follows:

$$\left[D^k_{ij}\right]\left[\phi^k_j(L)\right] = \left[S^k_{ij}\right]\left[\left(\frac{\partial\phi}{\partial n}\right)^k_j(L)\right] + \left[W^k_{ijl}(TE)\right]\left[\Delta\varphi^k_{ijl}(L)\right] \tag{12}$$

In actual numerical computation, the assembly of the matrices depends on the total number of panels and the source and dipoles coefficients. The method can be particularly time consuming particularly when the number of panels is large. For propeller of K blades with M panel dividing in radial and N panels in chordwise, the total equations system become $K \times M \times 2N$. Adding the hub, it becomes a large system of equations, which must be calculated for the propeller.

2-2-Iterative Pressure Kutta Condition

The Kutta condition (9) which requires that the pressure difference at the control points on the back and face sides of blade panels adjacent to the trailing edge should be zero can be expressed in the discretized form as;

$$\Delta p^k_j(L) = p^{k,B}_j(L) - p^{k,F}_j(L) = 0, \qquad j=1,2,..M \tag{13}$$

A direct solution of the resulting system of equations, (11) and (13) is difficult due to nonlinear features of equation (13). Therefore an iterative method is required to solve the system of equation (11) and satisfy equation (13). At the n^{th} iteration, we solve the linear system of equation (11) with the values of $\Delta\phi_j^k(L)$ determined from the $(n\text{-}1)^{th}$ iteration. The potential

The strength of the source distribution in equation (5) is known from kinematic boundary condition (KBC) as follows;

$$\frac{\partial \phi}{\partial n} = -\vec{V}_I(X,Y,Z,t).\vec{n} = -\left[V_S\left(1 - w(X,Y,X,t)\right) + \vec{\omega} \times \vec{r}(X,Y,X,t)\right]\vec{n} \tag{6}$$

where $\vec{n}$ denotes the outward normal unit vector

The strength of dipole distribution is unknown and equal to the perturbation potential on the propeller or to the potential jump in the trailing vortex wake. On the wake surface S_W, the velocity is considered to be continuous while the potential has a jump across the wake. It is expressed in the perturbation potential as,

$$\Delta\left(\frac{\partial \phi(r,t)}{\partial n}\right)_{S_W} = \left(\frac{\partial \phi(r,t)}{\partial n}\right)^B - \left(\frac{\partial \phi(r,t)}{\partial n}\right)^F = 0 \tag{7}$$

$$\left(\Delta\varphi(r,t)\right)_{S_W} = \phi^B(r,t) - \phi^F(r,t) = \Gamma(r,t) \tag{8}$$

where indexes B and F mean back and face sides of the propeller, respectively.

In the steady flow problem, the potential jump $\Delta\phi(q)$ is constant across the wake surface along an arbitrary streamline in the wake and its value is also constant with time, but when unsteady flow is streamed along the trailing wake and the value of the potential varies with time.

Another important physical boundary condition is the Kutta condition and its implementation. In lifting flows the circulation distributions on the lifting portions drives the entire solution. Accordingly, accurate determination of this circulation is crucial. Values of circulation are determined mainly from the Kutta condition along the trailing edges, and thus specifications of the Kutta condition is more important than any other detail of the numerical implementation.

The theoretical and physical form of the Kutta condition states that the velocity shall remain finite all along the sharp trailing edges. An equivalent alternative form may be imposed in the numerical solution such that equal pressure occurs the back and face surfaces of the trailing edge. This equal pressure Kutta condition will be applied to determine the unknown $\Delta\phi_{TE}$ of the dipole strength on the wake surface. In the numerical calculation, the pressure Kutta condition can be expressed as:

$$\Delta p_{TE}(r,t) = p_{TE}{}^B(r,t) - p_{TE}{}^F(r,t) = 0 \tag{9}$$

A direct solution of the resulting system of equations obtained from discretized Green's formula for the perturbation velocity potential (5), along with equation (9) is difficult due to the nonlinear character of the equation (5) therefore, an iterative solutions algorithm is employed to solve the problem. We focus on the numerical implementation in the following section.

2-Numerical Implementation

2-1-Discretization of the Propeller and Constitution of the Equations System

To solve the equation (5) numerically, we discretize the propeller and its trailing vortex wake surfaces into quadrilateral panels described in the reference [12]. The time domain is also

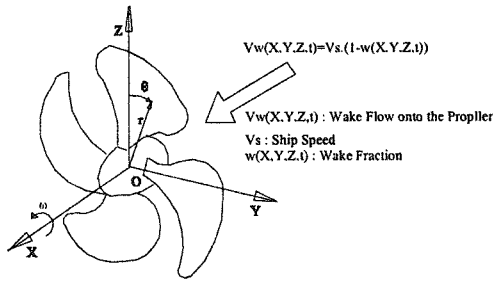

Figure (1) Coordinate system of marine propeller.

Denoting the components of the unsteady non-uniform velocity field towards the propeller in Cartesian coordinates by

$$\vec{V}_I(X,Y,Z,t) = \vec{V}_W(X,Y,Z,t) + \vec{\omega} \times \vec{r}(X,Y,Z,t) \tag{3}$$

The assumption at this point, is that the flow is incompressible and non-viscous. In addition, the wake velocity $V_W(x,y,z,t)$ is assumed to be the effective wake, which includes the interactions between the vorticities of the inflow with and without the propeller. Since there is currently no method for calculating the effective wake, the measured wake flow must be used to obtain the propeller performance. Having the measured wake flow $w(X,Y,Z,t)$ and ship's speed V_S, the flow velocities into the propeller due to wake are expressed as follows:

$$V_W(X,Y,X,t) = V_S(1 - w(X,Y,X,t)) \tag{4}$$

Notice that wake fraction in the reference are mostly given by some approximate formulae or measure data. It is noted that the wake field is strongly dependent on stern shape and so each ship can be considered to have a unique wake field.

1-1-Basic Formula

By applying Green's theorem for perturbation velocity potential $\phi(X,Y,Z,t)$ at any time, we can get the following integral equation on the propeller and its trailing vortex wake.

$$2\pi\phi(p) = \int_{S_B} \left\{ \phi(q) \frac{\partial}{\partial n_q}\left(\frac{1}{R(p;q)}\right) - \frac{\partial \phi(q)}{\partial n_q}\left(\frac{1}{R(p;q)}\right) \right\} dS + \int_{S_W} \Delta\varphi(q,t) \frac{\partial}{\partial n_q}\left(\frac{1}{R(p;q)}\right) dS \tag{5}$$

$R(p;q)$ is the distance from the field point p to the singularity point q. This equation may be regarded as a representation of the velocity potential in terms of a normal dipole distribution of strength $\phi(p)$ on the body surface S_B, a source distribution of strength $\partial\phi/\partial n$ on S_B, and a normal dipole distribution of strength $\Delta\phi(q,t)$ on the trailing wake surface S_W.

1-2-Boundary conditions

surface panels singularity distributions and boundary conditions. Most of the panel methods are based on the Douglas Newmann constant source method developed by Hess and Smith [20], in which the major unknown was the source strength which is determined from the boundary condition of requiring zero normal velocity at a control point on each panel. Another formula has arisen from the application of Green's Identity to determine the unknown potential strength. It was firstly introduced by Morino [10] for general lifting bodies in the field of wing theory.

In the past years, many researchers have applied this method to the marine propeller problems in steady flow (for example, Koyama [15], Hoshino [1][2], Kinnas [26] and Ghassemi [12]). However, predicting cavitation on marine propellers in unsteady flow, which is our main objective has not been reported yet. In the present paper, we have focused the simulation method on the unsteady propeller flow, before going ahead to achieve the prediction of cavitation. The same method has been employed for hydrofoil and propeller cavitation prediction in steady flow with satisfactory results [27]. Predicting cavitation in the unsteady flow is a challenging task which will be logical extension of the present method in the near future.

In this paper, a potential-based boundary element method is applied to the hydrodynamic analysis of marine propellers operating in non-uniform flow. Hyperboloidal quadrilateral panels with constant source and dipole distributions are used to approximate the surface of the propeller. An iterative pressure Kutta (IPK) condition (with special numerical techniques) has been applied to satisfy the equality of pressure at the trailing edge at each time step. In order to validate the numerical results, two propellers were selected to validate the method. One was a conventional propeller (CP) and the other was a highly skewed propeller (HSP). Steady and unsteady pressure distributions on each propeller were calculated by the present method and compared with experimental data for both model propellers and full-scale measurements by Ukon et al [18].

The remainder of the paper is organized as follows. Section 2 describes the mathematical formulation, boundary conditions and inflow wake velocity onto the propeller. Numerical implementation is explained in Section 3. Section 4 presents the computational results and compares them with experimental data for both steady and unsteady flows. We present conclusions in Section 5.

1-Mathematical Formulation

1-1-Wake flow velocity onto the propeller

In order to proceed with the boundary element method (BEM), the total unsteady velocity potential $\Phi(X,Y,Z,t)$ and the perturbation velocity potential $\phi(X,Y,Z,t)$ are related as follows:

$$\Phi(X,Y,Z,t) = \Phi_I(X,Y,Z,t) + \phi(X,Y,Z,t) \tag{1}$$

where $\Phi_I(X,Y,Z,t)$ is the local unsteady potential flow onto the propeller and it is expressed as;

$$\Phi_I(X,Y,Z,t) = \vec{V}_I(X,Y,Z,t).\vec{X}_P(t) \tag{2}$$

where $\vec{V}_I(X,Y,Z,t)$ and $\vec{X}_P$ are unsteady inflow velocity and position vector of the propeller, respectively.

The propeller is assumed to rotate with a constant angular velocity ω around the $X-$axis in the negative direction of θ, as depicted in Fig. 1.

Hydrodynamic Characteristics of Marine Propellers in Steady and Unsteady Wake Flows

Hassan Ghassemi
Assistant Professor
Department of Marine Technology,
Amirkabir University of Technology

Abstract

A marine propeller in unsteady wake flow is analyzed by using a potential-based boundary element method (BEM). Constant strength dipole and source distributions are used on each quadrilateral panels representing the propeller blades and their trailing vortex wakes. An analytical modification of Morino's method is adopted to determine the influence coefficients of source and dipole using hyperboloidal quadrilateral panels. This is very important for accuracy of the solutions. An iterative pressure Kutta (IPK) condition is applied to ensure pressure equality at the trailing edge of the blade. First, calculations were conducted for a steady flow to confirm the accuracy and the capability of the present method. Next, the calculations of the unsteady flow due to the ship's wake were performed to calculate the fluctuating pressure acting on the propeller and consequently the thrust and torque. The thrust fluctuation for one blade and the whole propeller are presented. The method is demonstrated for two propellers, one corresponding to the conventional propeller and one for a highly skewed. The unsteady pressure distributions on the propeller blades determined by the method are in good agreement with experimental data obtained from full-scale propellers.

Keywords

Hydrodynamic Performance, Pressure Distribution, Non-Uniform Wake, Unsteady Flows

Introduction

Marine propellers are usually operate in the region of disturbed flow, behind a ship. The non-uniform flow generates periodic, fluctuating pressure and as a result, vibratory forces can occur. The induced forces may transfer to the ship's hull through the shaft-line and fluid and the resulting vibrations are generally unpleasant and discomforts to the crews and passengers. The wake field is strongly dependent on hull shape and so each ship can be considered to have a unique wake field. It is a challenge for Naval Architects and Hydrodynamicists to predict the performance of the marine propellers working in a non-uniform wake field.

Modern research in computational hydrodynamics is linked to the development of the computer, and many numerical methods developed during the second half of the twentieth century. The potential-based boundary element method (BEM) is suitable for the analysis of configuration problems because it has good accuracy combined with low computational times. Many researchers have applied this method to wide variety of numerical predictions. As a result there has been some optimization of the method in order to achieve better and faster solution. There are a wide variety of potential-based panel methods, which employ different type of